Development and Characterization of Non-coated and PLGA-Coated S53P4 and S59 Bioactive Glass Scaffolds for Treatment of Load-Bearing Defects

Strömberg, Gustav; Aalto-Setälä, Laura; Uppstu, Peter; Björkenheim, Robert; Pajarinen, Jukka; Eriksson, Elin; Lindfors, Nina C.; Hupa, Leena

Published in:
Biomedical Materials and Devices

DOI:
https://doi.org/10.1007/s44174-023-00099-4

Published: 01/01/2023

Document Version
Final published version

Document License
CC BY

Biomedical Materials & Devices
https://doi.org/10.1007/s44174-023-00099-4

ORIGINAL ARTICLE

Development and Characterization of Non-coated and PLGA-Coated S53P4 and S59 Bioactive Glass Scaffolds for Treatment of Load-Bearing Defects

Gustav Strömberg[1] · Laura Aalto-Setälä[2] · Peter Uppstu[3] · Robert Björkenheim[1] · Jukka Pajarinen[1] · Elin Eriksson[4] · Nina C. Lindfors[1] · Leena Hupa[2]

Received: 6 March 2023 / Accepted: 6 June 2023

Abstract

We studied how in vitro reactions affect long-term biochemical and mechanical properties of porous tissue engineering scaffolds based on two bioactive glasses and accordingly their potential suitability for treating critical-size load-bearing bone defects. Granules of bioactive glass S53P4 and S59 were used to sinter the porous scaffolds. The sintering variables for mechanically durable scaffolds were initially selected according to the thermal behaviour of the glasses during heating. The S53P4 and S59 scaffolds were further divided into the following three groups: uncoated scaffolds, poly(DL-lactide-co-glycolide) (PLGA) coated scaffolds, and scaffolds coated with a mixture of PLGA and powdered S53P4. The purpose of the coating is to enhance mechanical abilities and to induce a membrane rich in growth factors surrounding the BAG implant. Characterization of the scaffolds included water absorption, pH, ion release, reaction layer formation, and compressive strength. Polymer coatings with powdered S53P4 absorbed more water than pure polymer coatings. The pH of the immersion solution increased more upon immersion of the uncoated scaffolds. No marked differences were seen between the coated scaffolds. During the 28-day in vitro immersion, the Ca-ion concentration initially increased for non-coated S53P4 scaffolds, followed by a slight increase starting at 14 days for all S53P4-based scaffolds and S59-PLGA scaffolds. The lowest P species concentration was observed for uncoated S53P4 scaffolds. The polymer coatings hindered the dissolution of Si-species from the scaffolds. Thicker calcium phosphate layers were identified at the uncoated scaffolds, suggesting a higher bioactivity. In contrast, the polymer coatings enhanced the compressive strength of the scaffolds. The results reflect the impact of glass composition and polymer coating on the chemical and physical properties of scaffolds, emphasizing the requirements in clinical applications for critical load-bearing bone defects.

Keywords Bioactive glass · Polymer · Dissolution · Bone graft substitute · Tissue engineering · Scaffold · Mechanical strength

Introduction

Bone tissue is classified as either compact cortical bone or spongy trabecular bone. The mechanical properties of bone tissue differ based on type and location. The compressive strength and porosity of cortical bone is 100–150 MPa and 5–10% respectively, compared with 2–12 MPa and 50–90% for cancellous bone [1]. These factors indicate the limits for the mechanical demands and surgical techniques for treating load-bearing defects with porous tissue-engineering scaffolds.

Loss of bone tissue due to, e.g., trauma, bone tumors, or infection may result in bone defects that require cavity filling, bone-supportive treatment, or both. In cavitary

✉ Gustav Strömberg
gustav.stromberg@helsinki.fi

✉ Nina C. Lindfors
nina.c.lindfors@hus.fi

1 Department of Hand, Ortopaedic and Traumatology and Plastic Surgery, Helsinki University Hospital, University of Helsinki, PL 3, 00014 Helsinki, Finland

2 Johan Gadolin Process Chemistry Centre, Åbo Akademi University, Henrikinkatu 2, 20500 Turku, Finland

3 Polymer Technology Research Group, Faculty of Science and Engineering, Åbo Akademi University, Henrikinkatu 2, 20500 Turku, Finland

4 Helsinki University, Helsinki, Finland

Published online: 04 August 2023

cancellous bone defects, the bone substitute is usually used as a stand-alone material, as the remaining cortical bone generates sufficient mechanical support. On the other hand, defects in cortical bone require mechanical support, which makes it more challenging to repair. Traditionally, surgical procedures on bone tissue are performed by supporting mechanical stability with plates, external fixators, or intramedullary nails, combined with autograft or allograft bone grafting if needed. Due to the limitations of autograft and allograft bone, the use of bone substitutes in repairing bone defects has become a standard procedure in many operations. Ideally, bone substitutes mimic the morphology and function of natural bone to integrate with surrounding tissues. In addition to an excellent biocompatibility, key requirements for an ideal and well-functioning bone substitute are macroscopic porosity enabling bone growth and vascularization and well-defined and suitable mechanical properties of the scaffold material [2, 3].

Bone substitutes based on bioactive glasses (BAGs) have been extensively studied and developed since this special family of glasses was discovered in the late 1960s [4]. Their suitability as bone-substitute materials comes from their verified bone-bonding properties and osteoconductive, bone growth, and vascular stimulatory properties [3–7]. Bonding of BAGs with bone has been described as a sequence of chemical reactions occuring at the glass surface. A rapid exchange of Na^+ and K^+ ions in the glass with H^+ and H_3O^+ from the extracellular solution occurs after implantation, leading to the formation of silanol (SiOH) groups at the glass surface and release of soluble silica in the solution. The silanol groups repolymerise into a silica-rich layer through which Ca^{2+} and PO_4^{3-} ions migrate and crystallise into a $CaO–P_2O_5$ hydroxyapatite (HA) layer on top of the silica-rich layer. Cell interactions with the HA layer then initiate the bone-forming pathway [6]. Today, BAGs are commercially used mainly as solitary granules or user-friendly putties for bone grafting under non-load-bearing conditions [6, 7].

When implanted in tissues and exposed to an extracellular fluid environment, BAGs gradually dissolve while supporting hydroxyapatite formation. Hench and co-workers observed that the controlled release of biologically active Ca and Si ions from BAGs induced upregulation and activation of seven families of genes in osteoprogenitor cells that accelerate bone regeneration [8]. However, the release rate of these inorganic ions from the BAG should be sufficiently high and persist over a critical period to stimulate and support tissue growth in the target application. Fundamentally, the ion release rate depends on the glass composition, while the actual ion concentrations in the interfacial solution also depend on the amount of the BAG, the BAG surface area ratio to the solution, and the flow rate of the solution. By suitably adjusting the oxide composition of the BAG, the type and concentration of ions released from the BAG can be tailored to elicit, e.g., both hydroxyapatite formation and vascularization of the growing new bone in vivo [2]. Changes in the BAG composition change the biochemical and physical properties of the materials, thus affecting its hot-working properties. Accordingly, the composition changes may have a notable impact on the mechanical properties on products manufactured through hot-working of glass. A set of desired properties of the BAG may be challenging to achieve as composition changes giving optimal property values for one particular property may lead to an undesired value for another property. For example, the low silica and high calcium oxide contents in BAGs challenge their hot-working into desired shapes through traditional methods without concurrent crystallization. If the glass crystallizes, the dissolution mechanisms and kinetics of the final product are different than those of the parent amorphous material. The clinically used BAG-S53P4 easily crystallizes during thermal treatments in a temperature window ranging roughly from 100 °C above the glass transformation temperature Tg (approximately 560 °C) and the liquidus temperature Tm (approximately 1230 °C), with surface crystallization as the predominant mechanism [9, 10]. Upon heating particles of S53P4, the temperature for the commencement of nucleation and crystal growth, Tx, is approximately 650 °C [11]. This roughly 100 °C temperature span between glass transformation and crystallization temperatures allows viscous-flow sintering of particles of S53P4 into porous 3D bodies. The sintering kinetics was suggested to overwhelm the crystallization kinetics of S53P4 and thus enable limited sintering through viscous flow between Tg and Tx [12]. However, the mechanical strength of the porous amorphous S53P4 scaffolds was low. When sintered at temperatures above Tx, the strength of the scaffolds gradually increased while the thickness of the partly crystallized layer at the surfaces grew [12]. The primary sintering occurred through viscous flow followed by the crystallization of the outer surfaces of the particles and the necks between the particles; the overall porosity of the scaffolds was not affected by the sintering temperature within the temperature range of 650–900 °C. These results implied that glass S53P4 can be sintered to partly crystalline porous scaffolds in such a way that the thickness of the crystallized layer is controlled and, accordingly, the amorphous bulk below the layer still exhibits the properties of the original glass. These results further imply that by properly optimizing the time–temperature schedule, BAG-S53P4 can be sintered into porous scaffolds with adequate strength required for surgery but with limited crystallization only, a feature that affects demands on commercial products.

Biodegradable biopolymer coatings have been used to improve the mechanical properties of BAG scaffolds [13]. However, the in vitro and in vivo properties are affected

by the polymer composition, its amount, and the coating method. The coating properties, such as the degradation rate, can also be modified, e.g., by choice of the molecular weight of the polymer or adjusting the monomer content and the end group composition [14–19]. The polymer coating may also affect the dissolution reactions of the BAG, e.g., by slowing down the reaction rate or affecting the pH of the surrounding media or solution [20].

BAG-S53P4 is clinically used as granules in ear, nose, and throat, cranio-maxillofacial, orthopedic, trauma, and spine applications [21–27]. The promising results from the sintering of melt-derived BAGs into porous scaffolds and applying biodegradable polymers to tune the properties of the scaffold for a particular application suggests that BAG applications can be extended into new areas of bone tissue engineering beyond their present bone grafting applications.

Poly(DL-lactide-co-glycolide) (PLGA) is an aliphatic copolyester manufactured by ring-opening polymerization of lactide and glycolide monomers. The properties of PLGA can be adjusted by altering the lactide-to-glycolide ratio. Compositions with a higher content of either lactide or glycolide degrade slower, whereas compositions close to a 50:50 ratio degrade faster [28]. Acidic end groups formed in the degradation may autocatalyze the degradation process inside the polymer matrix, thus increasing the degradation rate of the polymer [29]. Clinically, PLGA is used as a suture material (e.g. Vicryl®, Panacryl®, Polysorb®), in craniofacial fixation (RapidSorb®), and drug delivery (Lupron Depot®) [30].

In a previous study, we used PLGA as a degradable coating on S53P4 scaffolds [2]. The aim was to irritate the surrounding tissue with the presence and degradation of the polymer coating such that membranes rich with growth factors would be induced around the scaffold, thus facilitating bone regeneration. The PLGA-coated S53P4 scaffolds induced in vivo a membrane with an increased expression of VEGF and similar TNF expression as polymethylmethacrylate (PMMA). In addition, expression of several bone morphogenic proteins (BMP) was superior or similar to induced membranes of S53P4 and PMMA [2, 31].

This study aimed to obtain and fabricate non-coated and PLGA-coated BAG-based scaffolds for load-bearing conditions and to evaluate their chemical and biomechanical properties. The purpose of the quickly degrading PLGA coating is the 'positive' tissue irritation in a similar fashion as in the in vivo studies above, both through its presence and through its degradation products. In this study, we examined the in vitro properties of these scaffolds. The BAGs used for the scaffold sintering were the well-known bioactive glass S53P4 (BonAlive®) and a low-silica, slightly bioactive experimental composition, S59 [32].

Materials and Methods

Glass Melting

Analytical-grade reagents Na_2CO_3, $CaCO_3$, $2H_2OCaHPO_4$, H_3BO_3 (Sigma-Aldrich, Steinheim, Germany) and Belgian quartz sand with a low iron content were mixed to produce S53P4 and S59. The nominal oxide compositions of the glasses are shown in Table 1. The glasses were melted in-house at 1360 °C in a platinum crucible for 3 h, cast into a graphite mould, annealed at 520 °C for 1 h, and then cooled to room temperature in an annealing furnace. To ensure the homogeneity of the glass, the melting was repeated. The glass was then crushed and sieved into 300–500 µm sized granules and fine-grained particles (32–45 µm).

Manufacturing of Glass Scaffolds

The optimal temperature ranges for sintering amorphous or only partly crystalline scaffolds of the two glasses were estimated from thermal analyses of the fine-grained particles using differential scanning calorimetry (DSC, Netzch STA 441 F1 Jupiter) and hot stage microscopy (HSM, Misura 3.0, Expert System). In both methods, the particles were heated at (the rate of) 10 °C/min up to 1200 °C. The changes in the DSC graph, i.e., the energy content as a function of temperature and the changes in the HSM sintering graph were used to determine the glass transformation temperature (Tg), the temperature at which the crystallization commences (Tx), and the temperature at which the crystallization has its maximum value (Tp) (Fig. 1). The glass transformation temperature was taken from the inflection point of the endothermic peak in the DSC curve, Tx was taken as the commencement of the exothermic peak, and Tp was the maximum value of the same peak. Correspondingly, the sintering range of the glasses in the HSM graph was correlated with the temperature range from the first decrease in the sintering curve to the first constant value, i.e., plateau, on the HSM graph. Based on the thermal analyses, the temperature windows for viscous flow sintering are 520–650 °C for S53P4 and 550–710 °C for S59.

The glass granules were put in graphite forms and sintered in a nitrogen atmosphere as described by Fagerlund et al. [33]. Based on SEM images (not shown), sintering

Table 1 Nominal oxide compositions of BAGs S53P4 and S59 (wt%)

Glass	Oxide				
	SiO_2	Na_2O	CaO	P_2O_5	B_2O_3
S53P4	53	23	20	4	–
S59	59.7	25.5	11	2.5	1.3

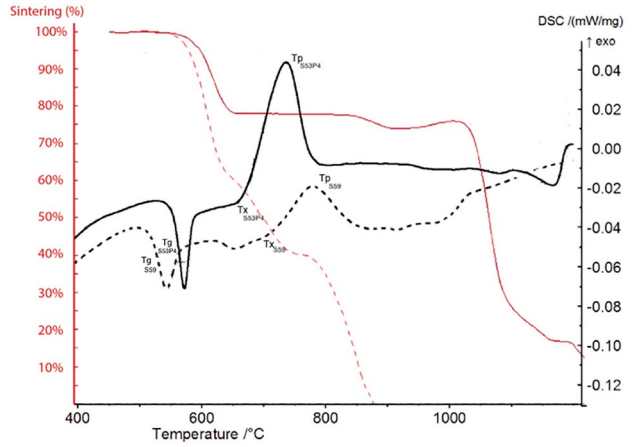

Fig. 1 Heating microscopy (red) and differential thermal analysis (black) curves for S53P4 (solid line) and S59 (dashed line)

of S53P4 at temperatures close to 700 °C resulted in scaffolds with a good neck between the granules and adequate mechanical strength. After thermal treatment at 700 °C, the surface of S53P4-based scaffolds is known to consist of a layer of $Na_2CaSi_2O_6$ crystals embedded in a residual glassy phase. This structure elicits hydroxyapatite formation at the glass surface in vitro [12]. After preliminary tests, the sintering temperature for the S53P4 scaffolds was selected just below the crystallization peak temperature, Tp (730 °C), to allow a viscosity level providing proper neck growth between the particles, desired overall porosity, and amorphous core below the crystallized surface layer.

S59 could be easily sintered into desired amorphous structures, but due to its rapidly decreasing viscosity with increasing temperature, the sintering temperature had to be carefully controlled to maintain the interconnecting porosity [34].

The final sintering time and temperature for the scaffolds were selected according to their apparent fragility in manual testing and on the pore size and interconnectivity revealed by the SEM micrographs of the scaffolds. Cylindrical scaffolds of a height of 10 mm and a diameter of 5 mm were sintered of both BAGs in a graphite mould in a nitrogen-filled oven for 90 min using 300–500 µm granules. The sintering temperature was 720 °C for S53P4 and 630 °C for S59.

Polymer Coating of BAG Scaffolds

The S53P4 and S59 scaffolds were divided into the following three groups: uncoated scaffolds (S53P4 and S59); scaffolds coated with an acid-terminated PLGA (S53P4-PLGA and S59-PLGA) and scaffolds coated with the PLGA mixed with amorphous powdered (32–45 µm) S53P4 (S53P4-PLGA + P, S59-PLGA + P). The powdered glass was added to include a highly bioactive component in the coating to enhance tissue formation. Further, a lactide monomer was added to this coating mixture to even out the pH increase by the glass powder, thus providing similar depolymerization conditions as for the polymer coating without glass powder.

The PLGA coating solution was prepared by dissolving 25% w/w acid-terminated low-molecular-weight PLGA (Purasorb PDLG 5002A, Corbion, Gorinchem, the Netherlands) in dichloromethane (DCM), after which the scaffolds were wholly immersed in the solution for 5 s which was sufficient to fill the porous glass scaffolds with the coating solution to yield the desired polymer coating. For the coating containing powdered S53P4, 10% w/w of glass powder to DCM and 1.5% w/w of L-lactide monomer were added to the PLGA coating solution. The coated scaffolds were dried overnight at room temperature in a fume hood and subsequently for 24 h in a vacuum oven at room temperature. The polymer coatings were distributed throughout the scaffolds. The coating masses were 42.8 ± 4.3 mg for S53P4-PLGA, 52.1 ± 5.1 mg for S53P4-PLGA + P, 32.9 ± 3.5 mg for S59-PLGA, and 37.9 ± 4.6 mg for S59-PLGA + P. In total, 183 scaffolds with and without coatings were prepared for the in vitro tests.

In Vitro Tests: Bioactivity, Water Absorption, pH, ICP-OES and SEM-EDXA

The in vitro bioactivity of the scaffolds was studied with static tests using simulated body fluid (SBF). The SBF solution was prepared according to the protocol proposed by Kokubo et al. [35]. Before the immersion, all scaffolds were sterilized using gamma irradiation with a dose of 25 kGy to provide similar conditions as bioactive glass-based samples used in vivo tests. The scaffolds were immersed at 37 °C in SBF for a predefined period of 1, 3, 7, 14, 21, or 28 days in an incubator (Stuart Orbital Incubator S 1500) rotated at a rate of 100 rpm. The scaffold mass-to-solution ratio was 3.5 mg/ml. The average mass (± standard deviation) was 347 mg (± 36 mg) for S53P4 and 372 mg (± 22 mg) for S59. Eight parallel scaffolds of each combination were tested for 7, 14, and 28 days: (1) uncoated, (2) coated with PLGA, and 3) coated with a mixture of PLGA, lactide, and BAG-S53P4 powder. In addition, three parallel scaffolds were tested for 1, 3, and 21 days. At each time point, the scaffolds were collected, superficially dried using tissue paper, and weighed to obtain the wet weight. The scaffolds were subsequently dried in a vacuum for at least 1 week and weighed. The change in weight was used to estimate the polymer's water absorption capacity. Uncoated scaffolds were used as a reference. Large differences in weight between the coated and uncoated scaffolds were interpreted as accelerated BAG dissolution, polymer degradation, or both. The pH of the incubation solution was measured after each dissolution period.

The concentrations of elements (Ca, P, and Si) released from the scaffolds into SBF were analyzed using ICP-OES (Optima 5300 DV; Perkin Elmer, Waltham, MA) as functions of the immersion time for three parallel samples and compared to an SBF reference solution without a scaffold. The reaction layers developed at the scaffold surfaces during the immersion were studied using SEM-EDXA (SEM, LEO 1530, Zeiss; EDXA Ultra Dry, Thermo Scientific).

Compression Strength

The compression strength is the maximum compressive stress that, under a gradually applied load, a given solid material can sustain without fracture. The formula for calculating compressive strength is:

$$\text{Compression Strength} = F / A$$

The compression strength was measured immediately after each immersion time in the wet condition for five parallel scaffolds. A polyurethane foam supportive sample holder was used to keep the scaffolds in an upright position during the testing. The compressive strength was measured under a compression rate of 2 mm/min using an L&W Crush Tester (Lorentzen & Wettre). Dry scaffolds before immersion were used as references.

Results

Water Absorption

The weight change of the scaffolds after each immersion time is shown in Fig. 2. The scaffolds were weighed wet after immersion and compared to the initial weight in the dry condition. Therefore, the weight change, given as % of the original sample weight, can be used to estimate the polymer's water absorption capacity. The uncoated scaffolds serve only as an additional reference. All coatings absorbed a significant amount of water. The coated S53P4 scaffolds showed a larger water absorption capacity than the coated S59 scaffolds, which was especially evident after 14 and 28 days of immersion. Further, the coating with embedded glass powder absorbed more water than the pure coating.

Changes in pH of Immersion Solutions

The increase in pH of SBF as a function of immersion time is shown in Fig. 3. The pH for S53P4 and S59 increased throughout the testing time, although the change was less for the S59-based samples. In contrast, the pH of SBF exhibited a declining trend over time for the coated scaffolds. For each measured time, the variation between the parallel samples was max ± 0.042 pH units.

Ion Release

The concentrations of Ca, P, and Si species in the solutions are presented in Fig. 4a–c. The high initial concentration of sodium in SBF prevented accurate measurement of the sodium ion release; thus, the data are not shown.

The initial release of Ca ions was highest for S53P4 than all other scaffolds (Fig. 4a). However, with increasing time, Ca concentrations showed an increasing trend for all scaffolds after 14 days of immersion. The Ca release was less from the S59 than from the other samples, as expected from the lower Ca content and the higher durability of S59.

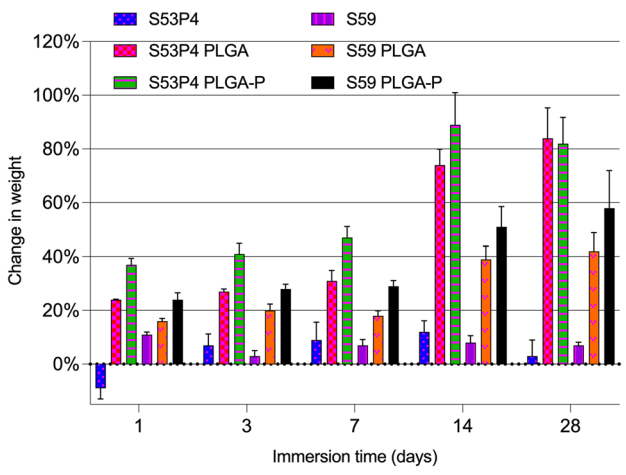

Fig. 2 Change in weight (%) over time (days) for uncoated and coated S53P4 and S59 scaffolds

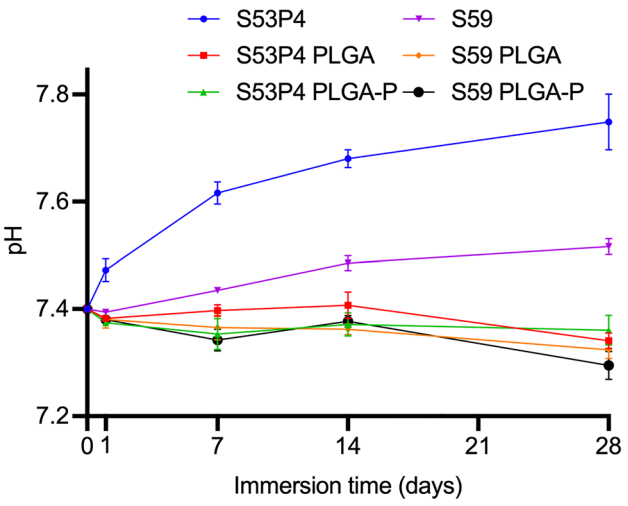

Fig. 3 pH change over time (days) after immersion in simulated body fluid (SBF) for uncoated and coated S53P4 and S59 scaffolds

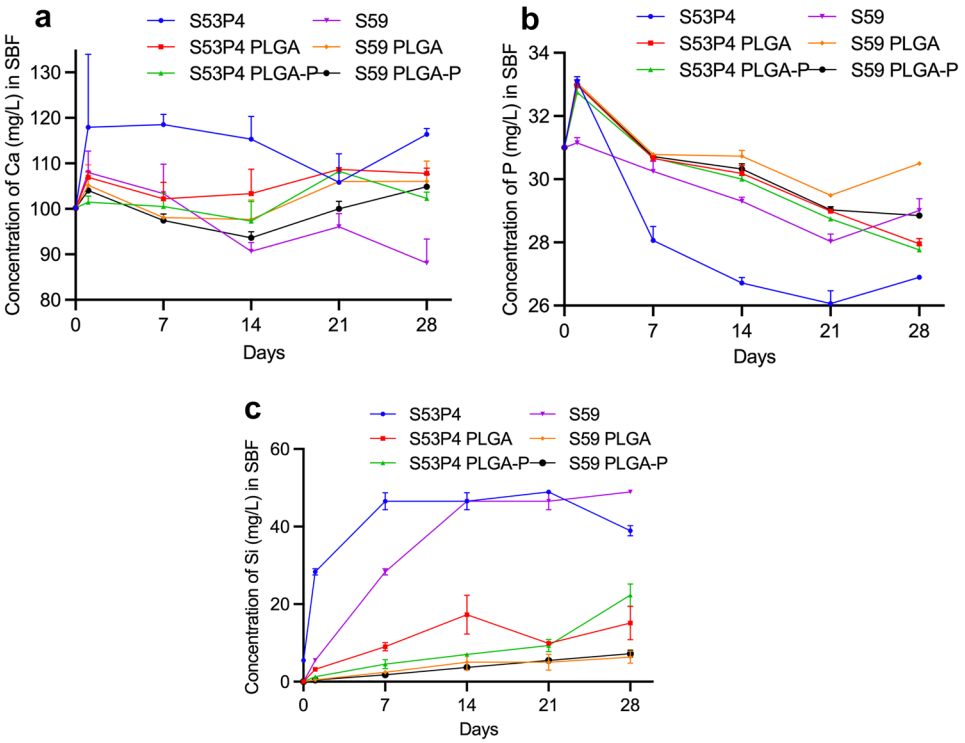

Fig. 4 **a**–**c** Average changes in concentration of **a** Ca, **b** P, and **c** Si in SBF as functions of immersion time for uncoated and coated S53P4 and S59 scaffolds. Values indicated are for three parallel samples

Except for S59, the concentration of the phosphorus species also increased significantly during the first day of immersion (Fig. 4b). This was followed by a gradual decrease except for S53P4, for which a significant decrease in phosphorus concentration was noted already between days 1 and 7.

In contrast to calcium and phosphorus, SBF does not contain silicon species initially. The concentration of Si species in SBF gradually increased throughout the immersion time for all scaffolds, with the highest levels observed for S53P4 and S59 (Fig. 4c). The dissolution of the Si species from the uncoated scaffolds stopped or strongly diminished with time. The silicon release plateaued after 7 days for the S53P4 scaffolds and after 14 days for the S59 scaffolds. The data for silicon species release from S59 correspond to typical Si-ion saturation concentration levels in SBF. Initially, the lowest concentrations of silicon species were observed for S53P4-PLGA-P, S59, and S59-PLGA.

Reaction Layer

The reaction layer formation was studied from cross-sectional areas of the scaffold struts. The S53P4 scaffolds developed a surface layer upon immersion in SBF. According to energy dispersive spectroscopy analysis, the Ca/P ratio in the layer corresponds to that of HA. The thickest and most widespread HA layer was observed on the uncoated scaffolds.

A thin HA layer also formed on the S59 scaffold joining the sintered granules in the interior parts of the scaffolds. These areas were assumed to experience limited ion diffusion to the bulk solution. No marked differences in the surface layer development were observed between the uncoated and the coated S59 scaffolds. SEM images of the cross-sections of S53P4 and S59 scaffolds after 1 and 28 days are shown in Fig. 5 (uncoated scaffolds), Fig. 6 (PLGA coated scaffolds), and Fig. 7 (PLGA-P coated scaffolds).

Compression Tests

Compression test data are presented in Fig. 8a, b. Compressive strength is equal to the maximum load (peak failure load) carried by the specimen during the test, divided by the average original cross sectional area.

A higher compression strength was observed for the coated than for the uncoated scaffolds. For S53P4-PLGA, the coating increased the compression strength more than the coating of S53P4-PLGA-P during the first hour of immersion. This effect decreased with longer immersion times. After 28 days of immersion, the coatings had a minor impact on compression strength (Fig. 8a).

For the S59 scaffolds (Fig. 8b), no clear differences between the coated and uncoated scaffolds were measured within the error margins. Generally, the S59 scaffolds showed a higher compression strength than the S53P4 scaffolds. Additionally, no apparent decrease in strength was measured for the S59 scaffolds during the 28 days of immersion.

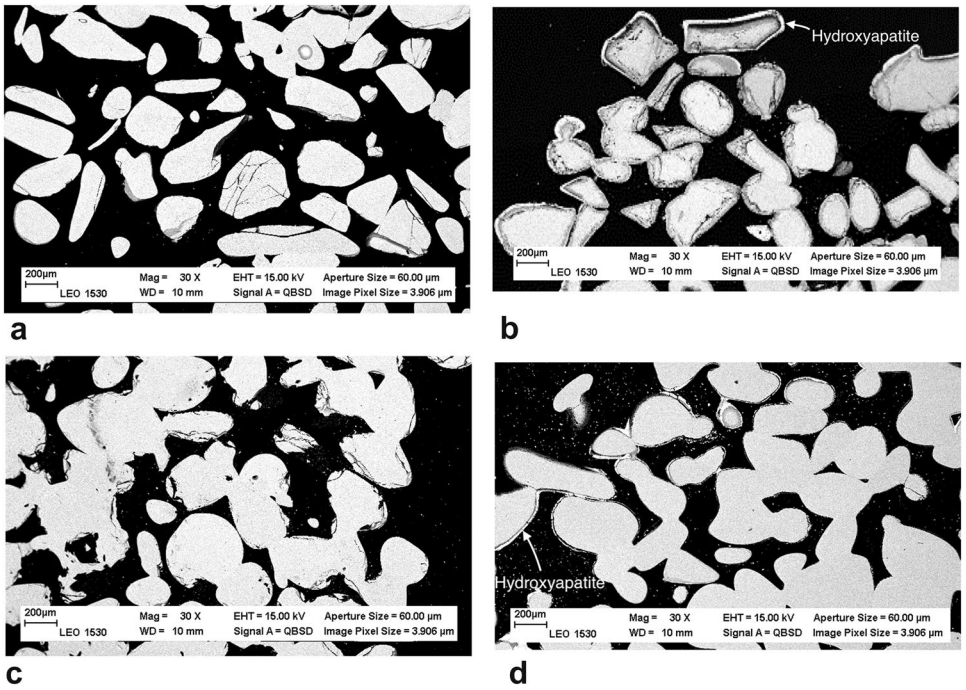

Fig. 5 SEM images of cross-sections of the uncoated scaffolds after immersion in SBF. **a** S53P4, 1 day, **b** S53P4, 28 days, **c** S59, 1 day, and **d** S59, 28 days

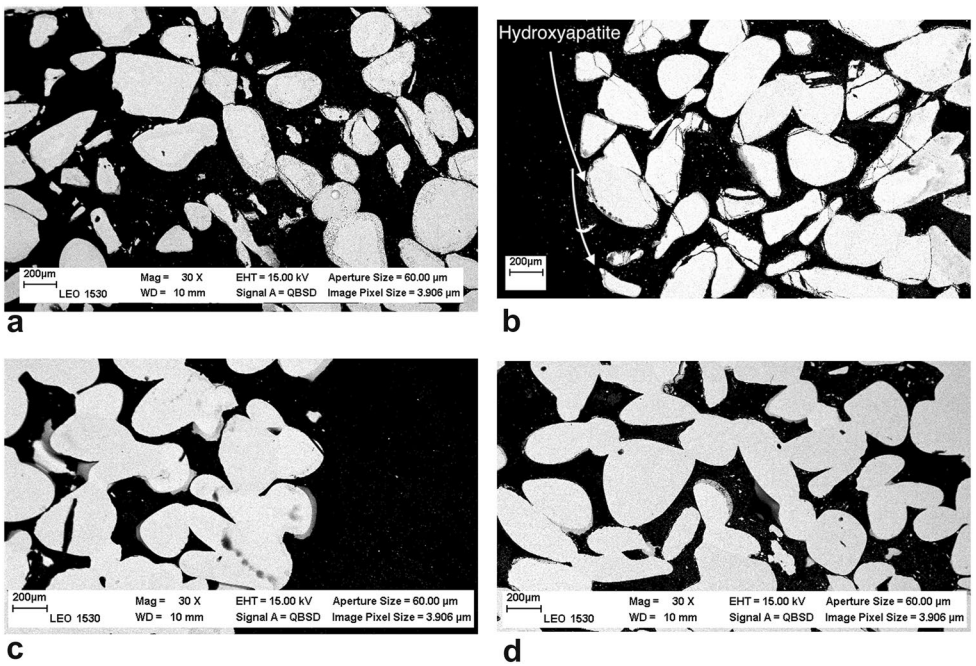

Fig. 6 SEM images of cross-sections of the PLGA-coated scaffolds after immersion in SBF. **a** S53P4-PLGA, 1 day, **b** S53P4-PLGA, 28 days, **c** S59P-PLGA, 1 day, and **d** S59P-PLGA, 28 days

Discussion

Bioactive glass S53P4 is a bone substitute with proven bone-stimulating, osteoconductive, angiogenic, and antibacterial properties [36, 37]. HA precipitation is commonly used to describe and compare the ability of a particular glass composition to form a chemical bond with bone and support bone regeneration. In this work, the in vitro properties of scaffolds sintered of two bioactive glasses, the well-known commercial S53P4 and one experimental glass S59 with and without polymer coatings based on the biodegradable polymer PLGA were compared after immersion in SBF for 28 days. SEM imaging (Figs. 5, 6 and 7) revealed that the cross-sections of the uncoated scaffolds of S53P4 developed a more significant

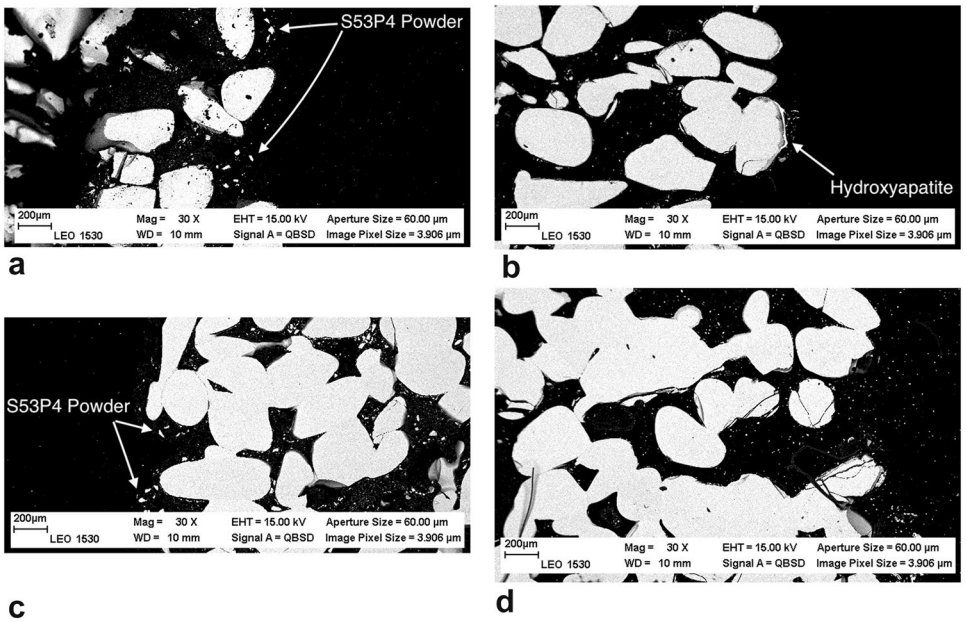

Fig. 7 SEM images of cross-sections of scaffolds coated with S53P4-PLGA-P. **a** S53P4-PLGA-P, 1 day, **b** S53P4-PLGA-P, 28 days **c** S59-PLGA-P, 1 day, and **d** S59PLGA-P 28 days

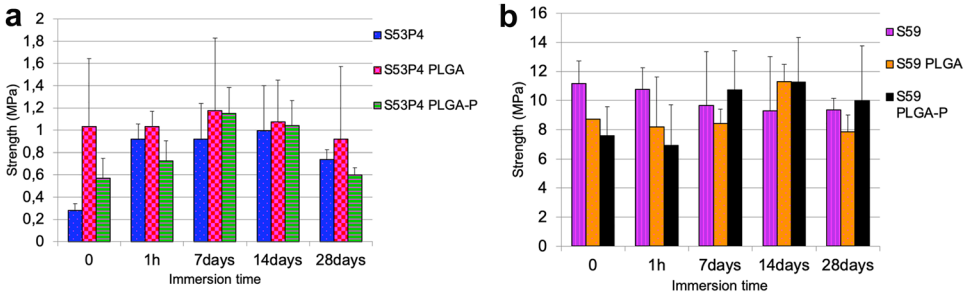

Fig. 8 Compression strength for coated and uncoated S53P4 (**a**) and S59 (**b**) after immersion in SBF

HA surface layer than the S59 scaffolds. This can be explained by the differences in the glass compositions. Although S59 develops a thin HA surface layer as reported by Lindfors et.al [32], its bioactivity is low. However, the S59 composition can easily be hot-worked into various products and its composition may be of interest for thin-walled products with a high surface area-to-volume ratio for enabling a desired overall ion release.

Phosphorus precipitation was more prominent in the case of uncoated compared to the coated scaffolds, implying a slower HA layer formation in the latter. This is seen in the SEM images of the uncoated S53P4 with a significant HA layer (Fig. 5). HA layer development is supported by the measured decrease in the phosphorus species concentration in SBF after 7 days of immersion. The uncoated scaffolds showed higher P species decrease than coated scaffolds, implying a faster HA layer formation (Fig. 4a).

In general, scaffolds based on S53P4 dissolve faster than scaffolds made of S59, as S59 is only slightly bioactive due to its high silica content [37, 38]. The greater release of Si from uncoated S59 than uncoated S53P4 is partly explained by its higher SiO_2 content and its lower bioactivity. As S59 has a higher silica content and gradually dissolves without an extensive condensation of Si species, the concentration of released Si in the solution ions is relatively high. In contrast, the condensation of Si–OH groups at the glass surface followed by the precipitation HA layer on S53P4 scaffolds may hinder further release of Si after the initial dissolution. Precipitation of HA within the silica-rich layer also retards dissolution of the glass [39]. In addition, the acidic environment that develops as a result of the degradation of the biodegradable polymer PLGA leads to a rapid dissolution of network-modifying ions from bioactive glasses [40]. Further, the dissolution of Si species is less in an acidic environment than in alkaline solutions.

The most notable difference in silicon release was not observed between the two glass compositions, but between uncoated and coated scaffolds based on the same glass. For uncoated scaffolds, the silicon species dissolution reached approximately 5% of the total amount over the immersion time, while for coated scaffolds the release ranged between 1 and 3%. In the static conditions tested, the silicon species

dissolution for S59 scaffolds approached a limit after 14 days and for uncoated S53P4 scaffolds after 7 days. However, for coated scaffolds the ion concentrations do not reveal whether the dissolution would have continued with longer immersion times. However, these results clearly show that the coating affected or retarded the dissolution, as was desired for further optimization of the biological responses in healing of critical load-bearing bone defects. Although the coating may act as a barrier to dissolution of the amorphous or partly crystallized scaffold, the acidic pH created by the degrading polymer is likely to markedly retard the release of Si species from the amorphous phase in the scaffolds while simultaneously creating an environment for supporting the structure of bone.

In our study, the coating had a significant effect on the pH of the in vitro solution. A decreasing trend in pH was measured for the coated scaffolds, in contrast to the uncoated S53P4 scaffolds for which the pH continued increasing throughout the test period. Thus, the network of the uncoated BAG-based scaffold continuously degraded, while the slowly degrading coated scaffolds provided structural support. The decreasing pH of the solution for the coated scaffolds may have a negative effect on antibacterial properties in vivo. The ion release with subsequent pH elevation is associated with reported antibacterial effects of BAGs [36]. Although the pH of the solution decreased for the coated scaffolds, concentrations of sodium, calcium, and phosphate ions increased in the solution with immersion time. Whether the increases in ion concentrations would as such affect the antibacterial properties is not clear, although the high concentrations of certain ions may participate in antibacterial properties [36]. A decrease in pH of the immersion solution for coated S53P4 and S59 scaffolds was likely due to polymer coating degradation. For uncoated scaffolds, the declining increase in pH after the formation of HA can be explained by the decrease in concentration of the phosphate/phosphorus species. This is in concordance with previous in vitro studies of powdered S53P4 (<45 µm) in SBF, according to which the pH elevation was greatest during the first 24 h. The ion release from powdered S53P4 showed a similar pattern for the phosphorus and calcium concentrations, namely a rapid increase in the beginning followed by a rather stable pH, and a decrease after 27 h of immersion due to HA formation [36].

Scaffolds coated with PLGA or PLGA mixed with powdered BAG-S53P4 absorbed a significant amount of water. Interestingly, coated S53P4 scaffolds absorbed more water than the coated S59 scaffolds. This may be due to the more bioactive nature of BAG-S53P4, which may affect polymer degradation [40]. The bonding between the polymer and bioactive glass also may be not strong enough to prevent the formation of capillaries and microcracks in the interface, thus leading to enhanced fluid diffusion [41, 42]. This fluid diffusion weakens the contact between the BAG and the polymer coating, increases surface area, and leads to an increase of water absorption. In water, PLGA degrades via hydrolysis of its ester linkages. Factors that affect the hydrolytic degradation of PLGA have been extensively studied [43].

Clinically, BAGs are used as granules in cavitary defects in low load-bearing conditions. To improve the mechanical properties and to increase the volume of bone substitutes in clinical use, mixtures of BAGs and autograft or allograft bone are often used. In a cadaveric porcine bone defect study that addressed the mechanical behaviour of BAG-S53P4 granules and morselized cancellous bone allograft of different volume mixtures, an equal volume mixture of BAG and allograft bone better met the clinical requirements for stability than BAG or allograft bone alone. In the study, highly controllable confined compression tests (CCT) and more clinically realistic in situ compression tests (ISCT) were used [44]. The same mixture also showed an aggregated modulus comparable to the stiffness of cancellous bone. BAG-S53P4 granules together with a synthetic binder, a so-called putty, is also gaining support among surgeons in the treatment of bone defects [45]. The relation between the putty composition and its mechanical behaviour has been evaluated in a study involving five different putty formulations, with variations in synthetic binder and granular content. Confined compression tests showed that impaction strain significantly decreased and the residual strain significantly increased with an increase of binder content. The stiffness of all five formulations was in the same range of that of cancellous bone [46].

The possible use of sintered, porous BAG scaffolds for the treatment of segmental load-bearing bone defects in more demanding clinical situations are likely limited due to low compression strength and low impaction strain of BAGs. However, other techniques, such as robocasting glass scaffolds of BAG-6P53B, yield a strength in the range of human cortical bone (100–150 MPa) [47]. In a comparative study of robocast BAG-45S5 scaffolds with various polymeric coatings, polymeric coating increased both mechanical strength and toughness of the BAG scaffolds. Chitosan-coated BAG-45S5 endured an axial strength up to 14 MPa, which decreased by 50% after 1 week of immersion in SBF [48]. Interestingly, the compresson strength of scaffolds of BAG-13-93 in SBF or implantation in vivo decrease during the first 2 weeks but more slowly thereafter. The brittle mechanical response in vitro changed an elasto-plastic response 2–4 weeks after implantation in vivo [49].

By changing the manufacturing process, granule size, and sintering temperature and by adding polymer coating, it is possible to alter the porosity and mechanical strength and bioactivity of the BAG-based scaffold and thus increase the mechanical properties of the final scaffold. However, optimizing the sintering conditions to achieve porous BAGs

with specific biological and mechanical properties is challenging. By studying the effect of sintering temperature on naturally derived hydroxyapatite for medical applications, the optimum sintering temperature for apatite growth and superior cell viability is 1300 °C, while maximum hardness was achieved at 1400 °C [42].

The scaffold should be sintered at a relatively low temperature to simultaneously maintain the bioactivity of BAG-S53P4 and hinder crystallization. On the other hand, low sintering temperatures may result in insufficient densification and very fragile scaffolds that are not in the mechanical range of human cortical bone. In our study, the mechanical properties of the scaffolds were clearly affected by the composition of the BAG and the PLGA coating. The PLGA coating had a positive effect on the axial mechanical strength, e.g. the coated S53P4 scaffolds were mechanically superior to uncoated S53P4 scaffolds before immersion in SBF. S59 scaffolds were less porous and had a significantly higher compressional strength than S53P4 scaffolds. Consequently, the effect of the coating and any possible HA layer formation on the surface of the scaffold would probably not have a significant effect on its axial mechanical strength. In our previous study, the biocompatibility of porous scaffolds based on the same glasses as in this study was tested using a rabbit in vivo model. The uncoated and PLGA-coated porous S53P4 scaffolds induced a foreign body induced membrane, with increased expression of VEGF and TNF and good expression of BMP-2, -4, and -7 when compared with membranes induced by PMMA, the gold standard method in clinical use [2, 31].

The mechanical properties of BAGs change oven time when the BAGs are in contact with body fluids. The mechanical properties of strong porous 13–93 scaffolds have been tested through compressive and flexural loading to determine strength, elastic modulus, fatigue resistance, and fracture toughness in vitro and in vivo. The compressive strength markedly decreased after 2 weeks of implantation in vivo or in SBF but more slowly thereafter. A statistically significant difference in compressive strength was not observed in vitro at 2, 4, and 6 weeks [48]. This is consistent with our results, in which the compressive strength of S53P4 first increased but decreased after 4 weeks of immersion in SBF. This decrease in compression strength was more evident for the coated scaffolds, which also had absorbed the most water at this time point, indicating polymer degradation. S53P4-PLGA generelly showed a slightly higher strength than S53P4-PLGA-P throughout the testing period. The latter also absorbed more water during the first 2 weeks of immersion. The rapidly reacting S53P4 powder was assumed to induce a faster local degradation of the polymer, resulting in higher water absorption and thus leading to a weaker mechanical support for the BAG scaffold. S53P4 showed a maximal compressive strength between the time intervals 1 h and 2 weeks of immersion. In contrast, the compressive strength remained quite constant throughout the SBF immersion for the uncoated and coated BAG-S59 scaffolds. A significant decrease in phosphorus concentration, suggesting HA precipitation, was measured for S53P4 during the 2 first weeks of immersion. The slight increase in the compressive strength of S53P4 up to 1 week was assumed to depend on HA precipitation (Fig. 8). At longer immersion periods, the continuous dissolution of the scaffolds (Fig. 4) likely weakened the necks between the granules and the strength decreased.

Conclusion

Partly crystalline scaffolds sintered of the well-known bioactive glass S53P4 and amorphous scaffolds of an experimental slowly reacting bioactive glass S59 with and without biodegradable PLGA coatings exhibited different in vitro behaviours. Scaffolds based on S53P4 dissolved faster than S59 scaffolds, thus showing a higher level of bioactivity. In contrast, S59 scaffolds dissolved slowly and retained their mechanical strength longer. The polymer coating increased the compression strength of scaffolds, but this effect faded with prolonged in vitro immersion as the coating degraded.

The in vitro tests of the sintered partly crystalline S53P4 scaffolds showed promising results for further in vitro and in vivo studies. The results suggest that it is possible to enhance mechanical properties, control ion dissolution rate, and thus optimize scaffold properties through biodegradable polymer coatings.

Funding Open Access funding provided by University of Helsinki including Helsinki University Central Hospital. The authors have no relevant financial or non-financial interests to disclose.

Data Availability The data that support the findings of this study are available from the corresponding author upon reasonable request.

Declarations

Conflict of interest On behalf of all authors, the corresponding author states that there is no conflict of interest.

References

1. K.A. Athanasiou, C. Zhu, D.R. Lanctot, C.M. Agrawal, X. Wang, Fundamentals of biomechanics in tissue engineering of bone. Tissue Eng. **6**, 361–381 (2000). https://doi.org/10.1089/107632700418083
2. R. Björkenheim, G. Strömberg, J. Pajarinen, M. Ainola, P. Uppstu, L. Hupa, T.O. Böhling, N.C. Lindfors, Polymer-coated bioactive glass S53P4 increases VEGF and TNF expression in an induced membrane model in vivo. J. Mat. Sci. **52**, 9055–9065 (2017). https://doi.org/10.1007/s10853-017-0839-6
3. L.L. Hench, The story of bioglass. J. Mater. Sci.: Mater. Med. **17**, 967–978 (2006). https://doi.org/10.1007/s10856-006-0432-z
4. L.L. Hench, J.R. Jones, Bioactive glasses: frontiers and challenges. Front. Bioeng. Biotech. **3**, 194 (2015). https://doi.org/10.3389/fbioe.2015.00194/full
5. J.K. Leach, D. Kaigler, Z. Wang, P.H. Krebsbach, D.J. Mooney, Coating of VEGF-releasing scaffolds with bioactive glass for angiogenesis and bone regeneration. Biomaterials **27**, 3249–3255 (2006)
6. D.S. Brauer, Bioactive glasses—structure and properties. Angew. Chem. Int. Ed. Engl. **54**, 4160–4181 (2015). https://doi.org/10.1002/anie.201405310
7. J.R. Jones, D.S. Brauer, L. Hupa, D.C. Greenspan, Bioglass and bioactive glasses and their impact on healthcare. Int. J. Appl. Glass Sci. **7**, 423–434 (2016). https://doi.org/10.1111/ijag.12252
8. L.L. Hench, Genetic design of bioactive glass. J. Eur. Ceram. Soc. **29**, 1257–1265 (2009)
9. H. Arstila, M. Tukiainen, S. Taipale, M. Kellomäki, L. Hupa, Liquidus temperatures of bioactive glasses. Adv. Mater. Res. **39**, 287–292 (2008)
10. L. Hupa, M. Hupa, S. Fagerlund, J. Massera, Crystallization mechanism of the bioactive glasses, 45S5 and S53P4. J. Am. Ceram. Soc. **95**, 607–613 (2012). https://doi.org/10.1111/j.1551-2916.2011.05012.x
11. H. Arstila, E. Vedel, L. Hupa, Hupa, M: Predicting physical and chemical properties of bioactive glasses from chemical composition. Part 2: Devitrification characteristics. Eur. J. Glass Sci. Technol. A **49**, 260–265 (2008)
12. S. Fagerlund, J. Massera, N. Moritz, L. Hupa, M. Hupa, Phase composition and in vitro bioactivity of porous implants made of bioactive glass S53P4. Acta Biomater. **8**, 2331–2339 (2012)
13. A. Philippart, A.R. Boccaccini, C. Fleck, D.W. Schubert, J.A. Roether, Toughening and functionalization of bioactive ceramic and glass bone scaffolds by biopolymer coatings and infiltration: a review of the last 5 years. Expert. Rev. Med. Dev. **12**, 93–111 (2014). https://doi.org/10.1586/17434440.2015.958075
14. F. Westhauser, C. Weis, M. Prokscha, L.A. Bittrich, W. Li, K. Xiao, U. Kneser, H.-U. Kauczor, G. Schmidmaier, A.R. Boccaccini, A. Moghaddam, Three-dimensional polymer coated 45S5-type bioactive glass scaffolds seeded with human mesenchymal stem cells show bone formation in vivo. J. Mater. Sci.: Mater. Med. **27**, 119 (2016). https://doi.org/10.1007/s10856-016-5732-3
15. W. Li, 45S5 bioactive glass-based composite scaffolds with polymer coatings for bone tissue engineering therapeutics, pp 15–17 (2015)
16. P. Nooeaid, W. Li, J.A. Roether, V. Mouriño, O.-M. Goudouri, D.W. Schubert, A.R. Boccaccini, Development of bioactive glass based scaffolds for controlled antibiotic release in bone tissue engineering via biodegradable polymer layered coating. Biointerphases **9**, 041001 (2014). https://doi.org/10.1116/1.4897217
17. B. Olalde, N. Garmendia, V. Sáez-Martínez, N. Argarate, P. Nooeaid, F. Morin, A.R. Boccaccini, Multifunctional bioactive glass scaffolds coated with layers of poly(d, l-lactide-co-glycolide) and poly(n-isopropylacrylamide-co-acrylic acid) microgels loaded with vancomycin. Mater. Sci. Eng. **33**, 3760–3767 (2013)
18. M. Peroglio, L. Gremillard, J. Chevalier, L. Chazeau, C. Gauthier, T. Hamaide, Toughening of bio-ceramics scaffolds by polymer coating. J. Eur. Cer. Soc. **27**, 2679–2685 (2007)
19. J. Yao, S. Radin, P.S. Leboy, P. Ducheyne, The effect of bioactive glass content on synthesis and bioactivity of composite poly (lactic-co-glycolic acid)/bioactive glass substrate for tissue engineering. Biomaterials **26**, 1935–1943 (2005)
20. M. Erol, A. Özyuğuran, Ö. Özarpat, S. Küçükbayrak, 3D composite scaffolds using strontium containing bioactive glasses. J. Eur. Ceram. Soc. **32**, 2747–2755 (2012)
21. J.T. Silvola, Mastoidectomy cavity obliteration with bioactive glass. Otolaryngology—Head Neck Surg **145**, 96–97 (2011). https://doi.org/10.1177/0194599811416318a176
22. A. Suomalainen, P. Stoor, K. Mesimäki, R.K. Kontio, Rapid prototyping modelling in oral and maxillofacial surgery: a two year retrospective study. J. Clin. Exp. Dent. **7**, e605 (2015)
23. N.C. Lindfors, I. Koski, J.T. Heikkilä, K. Mattila, A.J. Aho, A prospective randomized 14-year follow-up study of bioactive glass and autogenous bone as bone graft substitutes in benign bone tumors. J. Biomed. Mater. Res. B **94**, 157–164 (2010). https://doi.org/10.1002/jbm.b.31636
24. N.C. Lindfors, J.T. Heikkilä, I. Koski, K. Mattila, A.J. Aho, Bioactive glass and autogenous bone as bone graft substitutes in benign bone tumors. J. Biomed. Mater. Res. B **90**, 131–136 (2009)
25. K. Pernaa, I. Koski, K. Mattila, E. Gullichsen, J. Heikkila, A. Aho, N. Lindfors, Bioactive glass S53P4 and autograft bone in treatment of depressed tibial plateau fractures—a prospective randomized 11-year follow-up. J. Long. Term. Eff. Med. Implants **21**, 139–148 (2011)
26. J. Rantakokko, J.P. Frantzén, J. Heinänen, S. Kajander, E. Kotilainen, E. Gullichsen, N.C. Lindfors, Posterolateral spondylodesis using bioactive glass S53P4 and autogenous bone in instrumented unstable lumbar spine burst fractures. A prospective 10-year follow-up study. Scand. J. Surg. **101**, 66–71 (2012). https://doi.org/10.1177/145749691210100113
27. J. Frantzén, J. Rantakokko, H.T. Aro, J. Heinänen, S. Kajander, E. Gullichsen, E. Kotilainen, N.C. Lindfors, Instrumented spondylodesis in degenerative spondylolisthesis with bioactive glass and autologous bone: a prospective 11-year follow-up. J. Spinal Disord. Tech. **24**, 455–461 (2011)
28. P. Gentile, V. Chiono, I. Carmagnola, P.V. Hatton, An overview of poly(lactic-*co*-glycolic) acid (PLGA)-based biomaterials for bone tissue engineering. Int. J. Mol. Sci. **15**, 3640–3659 (2014)
29. C. Engineer, J. Parikh, A. Raval, Review on hydrolytic degradation behavior of biodegradable polymers from controlled drug delivery system. Trends Biomater. Artif. Organs. **25**, 79–85 (2011)
30. V.B. Damodaran, D. Bhatnagar, N.S. Murthy, *Biomedical polymers: synthesis and processing* (Springer, Cham, 2016). https://doi.org/10.1007/978-3-319-32053-3
31. R. Björkenheim, G. Strömberg, M. Ainola, P. Uppstu, L. Aalto-Setälä, L. Hupa, J. Pajarinen, N.C. Lindfors, Bone morphogenic protein expression and bone formation are induced by bioactive glass S53P4 scaffolds in vivo. J. Biomed. Mater. Res. B **107B**, 847–857 (2019). https://doi.org/10.1002/jbm.b.34181
32. N.C. Lindfors, P. Slätis, K.H. Karlsson, Ö. Andersson, Bone growth into surgically created cavities implanted with glass granules. Bioceramics **8**, 107–111 (1995)
33. S. Fagerlund, J. Massera, N. Moritz, L. Hupa, M. Hupa, Phase composition and in vitro bioactivity of porous implants made of bioactive glass S53P4. Acta. Biomater. **8**, 2331–2339 (2012). https://doi.org/10.1016/j.actbio.2012.03.011
34. E. Vedel, H. Arstila, H. Ylänen, L. Hupa, M. Hupa, Predicting physical and chemical properties of bioactive glasses from

chemical composition. Part 1. Viscosity characteristics. Glass Technol. Eur. J. Glass Sci. Technol. **49**, 251–259 (2008)
35. T. Kokubo, H. Kushitani, S. Sakka, T. Kitsugi, T. Yamamuro, Solutions able to reproduce in vivo surface-structure changes in bioactive glass-ceramic A-W3. J. Biomed. Mater. Res. **24**, 721–734 (1990)
36. D. Zhang, O. Leppäranta, E. Munukka, H. Ylänen, M.K. Viljanen, E. Eerola, M. Hupa, L. Hupa, Antibacterial effects and dissolution behavior of six bioactive glasses. J. Biomed. Mater. Res. A **93**, 475–483 (2010). https://doi.org/10.1002/jbm.a.32564
37. J.-C. Aurégan, T. Bégué, Bioactive glass for long bone infection: a systematic review. Injury **46**, 3–7 (2015)
38. H. Ylänen, K. Karlsson, A. Itälä, H.T. Aro, Effect of immersion in SBF on porous bioactive bodies made by sintering bioactive glass microspheres. J. Non-Cryst Solids **275**, 107–115 (2000)
39. O.H. Andersson, I. Kangasniemi, Calcium phosphate formation at the surface of bioactive glass in vitro. J. Biomed. Mater. Res. **25**, 1019–1030 (1991). https://doi.org/10.1002/jbm.820250808
40. L. Björkvik, X. Wang, L. Hupa, Dissolution of bioactive glasses in acidic solutions with the focus on lactic acid. Int. J. Appl. Glass Sci. **7**, 154–163 (2016). https://doi.org/10.1111/ijag.12198
41. L. Varila, T. Lehtonen, J. Tuominen, M. Hupa, L. Hupa, In vitro behaviour of three biocompatible glasses in composite implants. J. Mater. Sci.: Mater. Med. **23**, 2425–2435 (2012). https://doi.org/10.1007/s10856-012-4693-4
42. J. Rich, T. Jaakkola, T. Tirri, T. Närhi, A. Yli-Urpo, J. Seppälä, In vitro evaluation of poly(ε-caprolactone-co-DL-lactide)/bioactive glass composites. Biomaterials **23**, 2143–2150 (2002)
43. E. Vey, C. Rodger, J. Booth, M. Claybourn, A.F. Miller, A. Saiani, Degradation kinetics of poly(lactic-co-glycolic) acid block copolymer cast films in phosphate buffer solution as revealed by infrared and Raman spectroscopies. Pol. Degrad. Stab. **96**, 1882–1889 (2011)
44. D.J.W. Hulsen, J. Geurts, N.A.P. van Gestel, B. van Rietbergen, J.J. Arts, Mechanical behaviour of Bioactive Glass granules and morselized cancellous bone allograft in load bearing defects. J. Biomech. **49**, 1121–1127 (2016)
45. F. Baino, I. Potestio, Orbital implants: State-of-the-art review with emphasis on biomaterials and recent advances. Mater. Sci. Eng. C **69**, 1410–1428 (2016)
46. N.A.P. van Gestel, D.J.W. Hulsen, J. Geurts, S. Hofmann, K. Ito, J.J. Arts, B. van Rietbergen, Composition dependent mechanical behaviour of S53P4 bioactive glass putty for bone defect grafting. J. Mech. Behav. Biomed. Mater. **69**, 301–306 (2017)
47. Q. Fu, E. Saiz, M.N. Rahaman, A.P. Tomsia, Bioactive glass scaffolds for bone tissue engineering: state of the art and future perspectives. Mater. Sci. Eng. C **31**, 1245–1256 (2011)
48. M. Azadeh, S. Eqtesadi, A. Pajares, P. Miranda, Enhancing the mechanical and in vitro performance of robocast bioglass scaffolds by polymeric coatings: Effect of polymer composition. J. Mech. Behav. Biomed. Mater. **84**, 35–45 (2018)
49. X. Liu, M.N. Rahaman, G.E. Hilmas, B.S. Bal, Mechanical properties of bioactive glass (13–93) scaffolds fabricated by robotic deposition for structural bone repair. Acta Biomater. **9**, 7025–7034 (2013)